Transition from the Kondo effect to a Coulomb blockade in an electron shuttle*

Zhang Rong(张 荣), Chu Wei-Dong(楚卫东), Duan Su-Qing(段素青), and Yang Ning(杨 宁)†

Institute of Applied Physics and Computational Mathematics, Beijing 100088, *China*

(Received 6 May 2013; revised manuscript received 30 May 2013)

We investigate the effect of the mechanical motion of a quantum dot on the transport properties of a quantum dot shuttle. Employing the equation of motion method for the nonequilibrium Green's function, we show that the oscillation of the dot, i.e., the time-dependent coupling between the dot's electron and the reservoirs, can destroy the Kondo effect. With the increase in the oscillation frequency of the dot, the density of states of the quantum dot shuttle changes from the Kondo-like to a Coulomb-blockade pattern. Increasing the coupling between the dot and the electrodes may partly recover the Kondo peak in the spectrum of the density of states. Understanding of the effect of mechanical motion on the transport properties of an electron shuttle is important for the future application of nanoelectromechanical devices.

Keywords: quantum dot, electron shuttle, Kondo effect, Coulomb blockade

PACS: 73.23.Hk, 72.15.Qm, 73.63.Kv **DOI:** 10.1088/1674-1056/22/11/117305

1. Introduction

The Coulomb blockade[1] is a characteristic of the transport of a quantum dot when it is weakly coupled to source/drain electrodes and the charging energies are much greater than the contact and temperature induced broadening of the electron levels in the dot. The Kondo effect[2–4] occurs when the quantum dot is strongly coupled to the source and drain, and has been also observed in both molecule and carbon nanotube devices. The Kondo peak in the density of states (DOS) at the Fermi level is a consequence of the spin exchange between electrons in the leads and a localized unpaired electron in the quantum dot,[5–7] which manifests itself as a sharp zero-bias anomaly in low temperature tunneling conductance.

The fast development of experimental techniques in recent years has provided opportunities for controlling the mechanical motion of the quantum dot, such as metal grain[8,9] and single molecules[10] elastically suspended between a source and a drain electrode. Such "electron shuttle" devices[11] or so-called nonoelectromechanical devices exhibit novel properties and have great application potential in future molecular electronics devices and quantum information circuits. For studies of the mechanical properties of nanoelectromechanical devices, silicon nanobeams[12] and nanopillars have been investigated. For the studies of transport properties, the Coulomb blockade in a coupled silicon electron shuttle has been demonstrated at room temperature,[13] and the spin-polarized transport in a quantum dot shuttle has also been discussed.[14] In a Kondo regime, the time-dependent Kondo temperature and the single-electron transport in the "Kondo shuttle" have also been discussed.[15] The generalized master equation method[16] and nonequilibrium Green's function (NEGF) method[17] have been employed to investigate the transport properties of electron shuttles in both tunneling and shuttling regimes.

The NEGF formalisms are successfully developed to analyze electron transport through quantum dots coupled to the source and drain within the Coulomb blockade regime. Several theoretical techniques have also been developed in the past decade to study the Kondo effect in quantum dots, including the equation of motion (EOM),[18] renormalization group techniques,[19–21] the noncrossing approximation approach,[22–25] Fermi-liquid theory,[26] etc. The NEGF has also been generalized to study the cases with time-dependent tunneling between the dot and the electrodes.[27,28] However, the systematical studies of quantum dot shuttles within the Kondo regime are still very limited. Therefore, in this paper, we present the EOM of the NEGF with time-dependent tunneling in a quantum dot electron shuttle, and show the effect of the quantum dot's mechanical motion on the Kondo peak of the DOS.

The paper is organized as follows. In Section 2, we describe the model and present a general expression for the Green functions under the condition that the couplings between the dot and the reservoirs are time-dependent. The equation of motion method is used to calculate the nonequilibrium Green's functions. In Section 3, we discuss the effect of the time-dependent tunneling on the system's DOS, especially the transition from the Kondo to Coulomb-blockade-like DOS due to the dot's mechanical oscillation, followed by a summary in Section 4.

*Project supported by the National Natural Science Foundation of China (Grant No. 11204016).

†Corresponding author. E-mail: yang_ning@iapcm.ac.cn

© 2013 Chinese Physical Society and IOP Publishing Ltd

2. Model and method

As shown in Fig. 1, a quantum dot containing a localized electron coupling with the electrodes is modeled by an Anderson Hamiltonian[29,30]

$$H = \sum_{\beta\gamma\sigma} \epsilon_{\gamma\beta\sigma} c^{\dagger}_{\gamma\beta\sigma} c_{\gamma\beta\sigma} + \sum_{\sigma} E_{\sigma} c^{\dagger}_{\sigma} c_{\sigma} + U c^{\dagger}_{\uparrow} c_{\uparrow} c^{\dagger}_{\downarrow} c_{\downarrow} + \sum_{\gamma\beta\sigma} \tau^{*}_{\gamma\beta\sigma}(t) c^{\dagger}_{\gamma\beta\sigma} c_{\sigma} + \text{H.c.}, \quad (1)$$

where $\epsilon_{r\beta\sigma}$ are the single-electron energies in the electrode β ($\beta = \text{L},\text{R}$) for the electron states r and σ (the index σ labels spin-down and spin-up electrons corresponding to the left and right leads), $c^{+}_{r\beta\sigma}$ and $c_{r\beta\sigma}$ denote the creation and annihilation operators for the electrodes (leads), and $\epsilon_{r\beta\sigma}$ is assumed to be uniformly spaced in the range corresponding to the conduction band for both spin orientations. The spacing between two adjacent levels in the electrode is typically set to be 10^{-4} of the bandwidth of the conduction band. In addition, c^{+}_{σ} and c_{σ} are the creation and annihilation operators for the electrons in the dot, $E_{\sigma} = E_0$ is the energy of the single dot level, and the energy U is the Coulomb interaction of electrons in the dot. We solve the problem within the low temperature regime, so U is chosen to exceed the thermal energy kT greatly. The last term describes the coupling of the reservoirs to the dot.

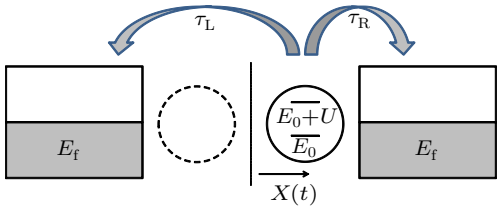


Fig. 1. The sketch of the quantum dot electron shuttle.

For traditional quantum dot systems, $\tau_{\gamma\beta\sigma}$ is usually assumed to be time-independent. For the quantum dot shuttle, we assume that the dot oscillates periodically between the two electrodes with frequency ω and the position of the dot $x(t) \propto \sin \omega t$. Then, the coupling or the tunneling of the electron between the dot and the left (right) electrode will be proportional to e^{-x} (e^{x}), respectively. We just choose the form $\tau_{\gamma L\sigma}(t) = \tau_0 \exp(-\sin(wt))$ and $\tau_{\gamma R\sigma}(t) = \tau_0 \exp(\sin(wt))$ in this paper, where τ_0 is a constant. In this model, when $t = 0$, the dot is in the middle of the two electrodes with the same coupling τ_0. As the dot moves to one electrode, the coupling between them will increase simultaneously, while the coupling to another electrode will decrease. Of course, if $w = 0$, the problem returns to the statistic case. It is worthwhile to note that similar time-dependent coupling may also be realized in an experiment with two alternately varied barriers between the dot and the electrodes.

When the coupling $\tau_{\gamma\beta\sigma}$ is time-independent, the EOM of the NEGF has been discussed in previous studies which revealed the transition from the Coulomb blockade to the Kondo regime in the electron transport when the coupling is gradually strengthened.[31] When the coupling is time-dependent, the Green's functions are not easy to obtain. With appropriate approximation in the high-order Green's functions, we can obtain the following EOM for the Green's functions in the case of time-dependent coupling.

For each spin channel, we introduce

$$G^{\gamma}_{\sigma}(t,t_1) = -\text{i}\Theta(t-t_1)\langle\{c_{\sigma}(t); c^{\dagger}_{\sigma}(t_1)\}\rangle,$$

and

$$G^{\gamma}_{\sigma}(E,t_1) = \langle\langle c_{\sigma}(t); c^{\dagger}_{\sigma}(t_1)\rangle\rangle = -\text{i}\int_{t_1}^{\infty} \langle\{c_{\sigma}(t); c^{\dagger}_{\sigma}(t_1)\}\rangle \, \text{e}^{\text{i}E(t-t_1)} \, \text{d}t.$$

Then, we can obtain

$$(E - E_0)\langle\langle c_{\sigma}; c^{\dagger}_{\sigma}\rangle\rangle = 1 + \sum_{\gamma\beta} \widehat{\tau_{\gamma\beta\sigma}} * \langle\langle c_{\gamma\beta\sigma}; c^{\dagger}_{\sigma}\rangle\rangle + U\langle\langle n_{-\sigma} c_{\sigma}; c^{\dagger}_{\sigma}\rangle\rangle, \quad (2)$$

$$(E - \epsilon_{\gamma\beta\sigma})\langle\langle c_{\gamma\beta\sigma}; c^{\dagger}_{\sigma}\rangle\rangle = \widehat{\tau_{\gamma\beta\sigma}} * \langle\langle c_{\sigma}; c^{\dagger}_{\sigma}\rangle\rangle, \quad (3)$$

and

$$\begin{aligned}
&(E - E_0 - U)\langle\langle n_{-\sigma} c_{\sigma}; c^{\dagger}_{\sigma}\rangle\rangle \\
&= \langle n_{-\sigma}\rangle + \sum_{\gamma\beta}\Bigg\{ \widehat{\tau_{\gamma\beta\sigma}} * \Bigg(\frac{\widehat{\tau^{*}_{\gamma\beta\sigma}} * \langle\langle n_{-\sigma} c_{\sigma};\, c^{\dagger}_{\sigma}\rangle\rangle}{E - \epsilon_{\gamma\beta\sigma}} \Bigg) \\
&\quad + \widehat{\tau_{\gamma\beta-\sigma}} * \Bigg(\frac{\widehat{\tau^{*}_{\gamma\beta-\sigma}} * \langle\langle n_{-\sigma} c_{\sigma};\, c^{\dagger}_{\sigma}\rangle\rangle}{E - \epsilon_{\gamma\beta-\sigma}} \Bigg) \\
&\quad - \widehat{\tau_{\gamma\beta-\sigma}} * \Bigg(\frac{\widehat{\tau^{*}_{\gamma\beta-\sigma}} * (f^{\beta}_{\gamma-\sigma}\langle\langle c_{\sigma};\, c^{\dagger}_{\sigma}\rangle\rangle)}{E - \epsilon_{\gamma\beta-\sigma}} \Bigg) \\
&\quad - \widehat{\tau^{*}_{\gamma\beta-\sigma}} * \Bigg(\frac{\widehat{\tau_{\gamma\beta-\sigma}} * (f^{\beta}_{\gamma-\sigma}\langle\langle c_{\sigma};\, c^{\dagger}_{\sigma}\rangle\rangle)}{E - 2E_0 - U + \epsilon_{\gamma\beta-\sigma}} \Bigg) \\
&\quad + \widehat{\tau^{*}_{\gamma\beta-\sigma}} * \Bigg(\frac{\widehat{\tau_{\gamma\beta\sigma}} * \langle\langle n_{-\sigma} c_{\sigma};\, c^{\dagger}_{\sigma}\rangle\rangle}{E - 2E_0 - U + \epsilon_{\gamma\beta-\sigma}} \Bigg) \Bigg\}, \quad (4)
\end{aligned}$$

where $\widehat{f}$ denotes the inverse Fourier transform of f, and $g * h$ denote the convolution of g and h.

For the situation that the time tends to be infinity, we introduce

$$A_{\text{L/R}}(\epsilon, t\to\infty) = \lim_{t\to\infty} \int_{-\infty}^{t} u_{\text{L/R}}(t_1) G^{r}_{\sigma}(t,t_1) \, \text{e}^{\text{i}\epsilon(t-t_1)} \, \text{d}t_1,$$

where $u_{\text{L}}(t) = \exp(-\sin(wt))$ and $u_{\text{R}}(t) = \exp(\sin(wt))$. Then, the mean occupation number of the dot is

$$\langle n_{\sigma}\rangle = \sum_{\text{L/R}} \frac{1}{2\pi} \int \text{d}\epsilon \Gamma^{\text{L/R}}_{\sigma}(\epsilon) f_{\text{L/R}}(\epsilon) |A_{\text{L/R}}(\epsilon, t\to\infty)|^2, \quad (5)$$

where $f_{\text{L/R}}(\epsilon)$ is the Fermi distribution function of the left/right electrode, and

$$\Gamma^{\beta}_{\sigma} = -2\text{Im}(\Sigma^{\beta}_{0\sigma}),$$

$$\Sigma^{\beta}_{0\sigma} = \frac{|\tau_{\gamma\beta\sigma}|^2}{E - \epsilon_{\gamma\beta\sigma}}.$$

See the Appendix for detailed derivations and the notations.

We initialize a $\langle\langle c_\sigma;\ c_\sigma^\dagger\rangle\rangle$, and the Green's functions with time-dependent coupling are obtained by using a self-consistent iterative procedure from Eq. (2) to Eq. (4). Then, the electron DOS in the dot can be found by

$$D(\epsilon) = -\frac{1}{\pi}\Sigma_\sigma \mathrm{Im}\left[G_\sigma^r(\epsilon)\right]. \quad (6)$$

The zero-bias conductance of the system can be also calculated using a Landauer formula,[32]

$$G = \frac{e^2}{h}\sum_\sigma \int \mathrm{d}\epsilon f'(\epsilon)\frac{2\Gamma_\mathrm{L}(\epsilon,t)\Gamma_\mathrm{R}(\epsilon,t)}{\Gamma_\mathrm{L}(\epsilon,t)+\Gamma_\mathrm{R}(\epsilon,t)}\mathrm{Im}\left[G_\sigma^r(\epsilon)\right], \quad (7)$$

where $f'(\epsilon)$ is the derivative of the Fermi distribution function.

3. Results and discussion

In this work, we choose $E_0 = -0.2$ eV, $U = 0.5$ eV, and $kT = 0.00026$ eV, making sure that the Coulomb energy is significantly larger than the thermal energy. The Fermi energy of the electrodes is set to $E_\mathrm{f} = 0$ eV.

Firstly, using Eq. (6), we present the equilibrium electron DOS of the system with $\omega = 0$ and $\tau_0 = 0.2$ eV in Fig. 2(a), where the EOM of the NEGF in Eqs. (2)–(4) goes back to the stationary case.[31] It can be found that the DOS exhibits an obvious Kondo effect feature, i.e., a sharp Kondo peak lies at $E = E_\mathrm{f} = 0$ eV. The mean electron occupation number of dots is 0.89 (sum of the mean numbers of the two spin orientations), which is very close to 1 and ensures that the Kondo effect can be manifested. For such a DOS, the electron transport channel will be the Kondo resonant tunneling. With the increase in the oscillation frequency ω, from Figs. 2(b) and 2(c) it can be found that the Kondo peak in the DOS is gradually damped. For $\hbar\omega = 10$ eV, there is still a tiny Kondo peak at $E = 0$ eV. For $\hbar\omega = 20$ eV, the Kondo peak completely disappears. With the fading away of the Kondo peak, two peaks at $E = E_0 = -0.2$ eV and $E = E_0 + U = 0.3$ eV gradually arise, which manifests the Coulomb blockade feature. For such a DOS, the electron transport will be mainly mediated by the shuttling of the dot with the charge and uncharge process. The in-depth understanding of the transport properties of a quantum dot shuttle within the shuttling regime is beyond the scope of the present paper, but worthwhile for future studies.

Although the mechanical oscillation of the quantum dot shuttle may destroy the Kondo resonance peak, increasing the coupling τ_0 may partly recover it if the oscillation frequency ω is not very large. In Fig. 3, we show the τ_0-dependent DOS of the quantum dot shuttle with fixed $\hbar\omega = 10$ eV and $\hbar\omega = 20$ eV. For small ω, as shown in Fig. 3(a), the DOS peaks lie at $E = E_0$ and $E = E_0 + U$ when $\tau_0 = 0.1$ eV. The heights of the two peaks at E_0 and $E_0 + U$ are not equal. This is because the mean occupation number of the dot is not 0.5. When τ_0 increases to 0.3 eV, the Kondo peak at $E = E_\mathrm{f} = 0$ eV is completely recovered as shown in Fig. 3(c). However, at this time, the mean occupation number of the dot is merely 0.57 (sum of the mean numbers of the two spin orientations) and the height of the Kondo peak is lower than that of the statistic case in Fig. 2(a).

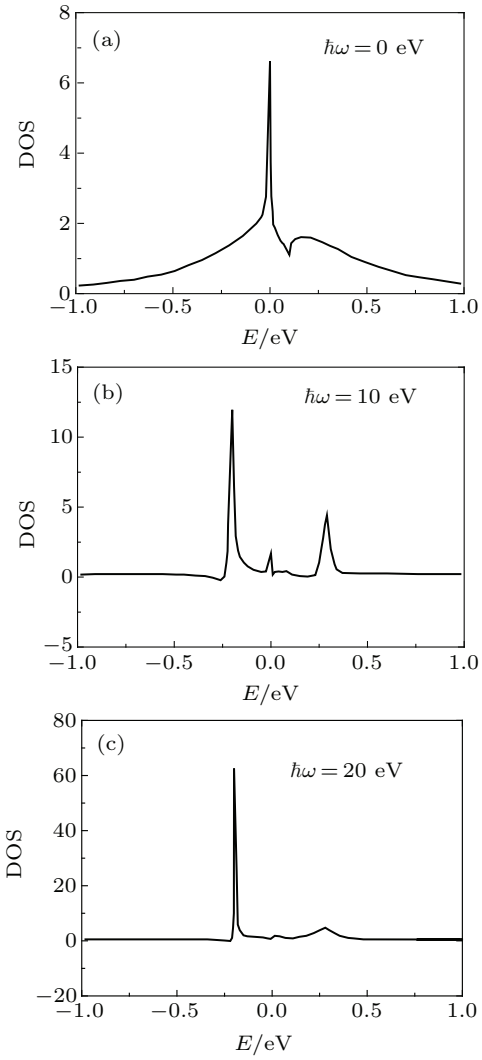


Fig. 2. The equilibrium electron density of states (DOS) with the coupling $\tau_0 = 0.2$ eV and $\hbar\omega = 0$ (a), 10 eV (b), and 20 eV (c).

However, for $\hbar\omega = 20$ eV, the Kondo peak is still a tiny feature in the DOS and the main peaks are still Coulomb-blockade like when $\tau_0 = 0.3$ eV, as shown in Fig. 3(b). The Coulomb blockade peaks are completely damped only when τ_0 increases to 0.5 eV. With such large tunneling, $\tau_0 \sim U$, the DOS feature is quite different from those with $\tau_0 < U$. Although a Kondo-like peak can be still resolved in Fig. 3(d), the height of the peak at $E = E_\mathrm{f} = 0$ eV is smaller than those in Fig. 3(c), and the whole DOS exhibits a wide spectrum. In fact, the DOS will be neither Coulomb-blockade-like nor Kondo-like when $\tau_0 > U$, but will be broadened to a wide range with a smooth form. This indicates that the quicker the dot oscillates, the more severely the Kondo effect be broken. If the dot oscillates too quickly, the Kondo effect may not be recovered even when the coupling τ_0 exceeds the Coulomb energy U.

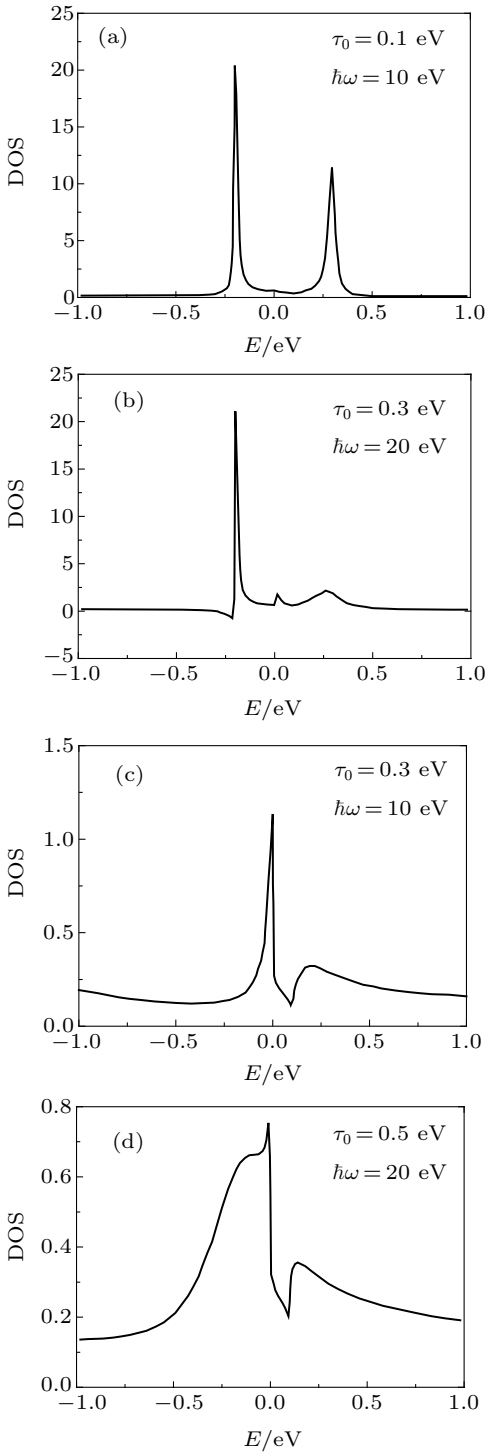


Fig. 3. The equilibrium electron density of states (DOS) with (a) $\hbar\omega = 10$ eV and $\tau_0 = 0.1$ eV, (b) $\hbar\omega = 20$ eV and $\tau_0 = 0.3$ eV, (c) $\hbar\omega = 10$ eV and $\tau_0 = 0.3$ eV, and (d) $\hbar\omega = 20$ eV and $\tau_0 = 0.5$ eV. In the calculations, $E_0 = -0.2$ eV, $U = 0.5$ eV, and $kT = 0.00026$ eV.

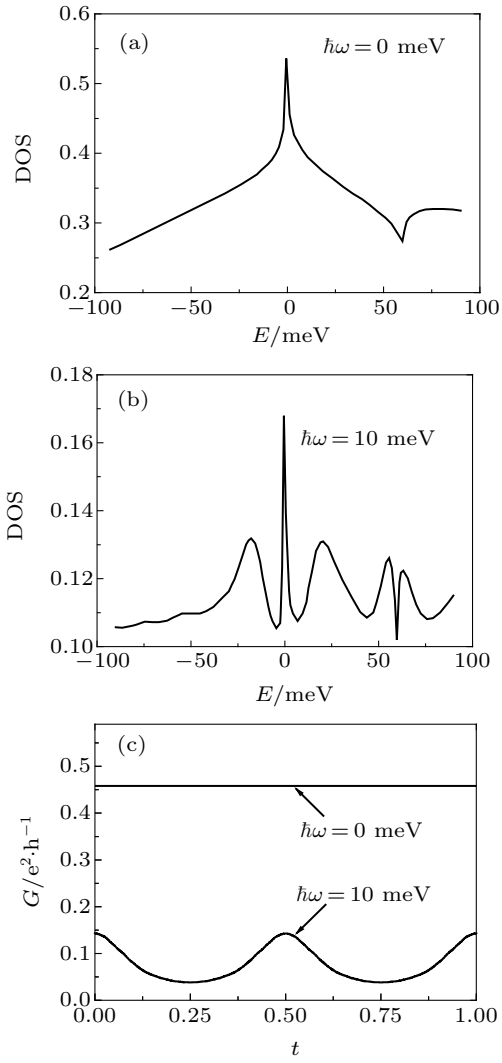


Fig. 4. The equilibrium electron density of states with (a) $\hbar\omega = 0$ meV and (b) $\hbar\omega = 10$ meV, and (c) corresponding zero-bias conductance (G) as a function of time. In the calculations, $E_0 = -20$ meV, $U = 100$ meV, $\tau_0 = 50$ meV, and $KT = 0.026$ meV.

Before ending the discussion, it is worthwhile giving some advice on the observation of the effect of the mechanical oscillation on the transport properties of an electron shuttle. The above discussion based on the prototype model suggests that the transition from the Kondo effect to Coulomb blockade occurs when the time scale of the mechanical oscillation is much smaller than that of the electron tunneling by the Kondo resonance, i.e., the frequency of the mechanical oscillation, is much quicker than the tunneling of the electron. However, the effect of the mechanical motion, such as the decrease of the Kondo peak, may be observed even with much slower oscillation. For the up-to-date electron shuttle devices based on the semiconductor quantum dots, the frequency of the mechanical oscillation can only reach hundreds of MHz, and the electron tunneling in the Kondo regime is still much quicker than this mechanical motion. For an electron shuttle based on molecular transistors, the energy scale of the electron tunneling is about several tens of meV or even above, and the Coulomb energy is several hundreds of meV. In addition, the Kondo effect has been observed in molecular transistors.[33,34] The most important feature of the electron shuttle based on molecular transistors is that its mechanical oscillation can reach THz range. For example, the centre-of-mass oscillation energy of a C_{60} molecule within the confinement potential that binds it to the gold surface can reach 5 meV (1.2 THz),

and its internal vibration energy can exceed 30 meV.[35] Such frequency of the mechanical motion may provide the opportunity to observe its influence on the Kondo effect. Thus, in Fig. 4, we calculate the DOS and the zero-bias conductance of an electron shuttle with $\tau_0 = 50$ meV, $U = 100$ meV, and $\hbar\omega = 0$ and 10 meV, respectively. It can be found that although the mechanical oscillation with $\hbar\omega = 10$ meV cannot make the transition from the Kondo effect to Coulomb blockade, it can indeed reduce the Kondo peak in the DOS. Such reduction is manifested in the zero-bias conductance. As shown in Fig. 4(c), the periodical zero-bias conductance is greatly reduced by the mechanical oscillation. The complete observation of the transition from the Kondo effect to Coulomb blockade may be achieved in some kind of nanomechanical single molecule devices with smaller mass or a larger force constant, which causes a larger oscillation frequency.

4. Summary

In summary, by deriving the equations of motion for the nonequilibrium Green's function with the time-dependent coupling between the dot and the electrodes, we have investigated the effect of the mechanical motion on the density of states of the quantum dot electron shuttle. It is clearly shown that the oscillation of the dot can induce the transition of the DOS from the Kondo-like to Coulomb-blockade pattern. Such transition may be partly reversed by increasing the coupling. However, for an oscillation with too large frequency, the Kondo-like DOS may be unrecoverable. The studies on the effects of the mechanical motion on the DOS of the electron shuttles provide the basis for the further investigation on the transport properties of nanoelectromechanical devices. Considering the typical energy scale of the electron tunneling and the mechanical oscillation, the electron shuttle based on the single-molecule transistors has been suggested to observe the influence of the mechanical oscillation on the Kondo peak.

Appendix

In this section, we will derive the equation of motion for the Green's function of the quantum dot electron shuttle.

For each spin channel, the retarded Green's function is

$$G^{\gamma}_{\sigma}(t,t_1) = -\mathrm{i}\Theta(t-t_1)\langle\{c_\sigma(t);c^{\dagger}_{\sigma}(t_1)\}\rangle,$$

and its Fourier component is

$$\begin{aligned} G^{\gamma}_{\sigma}(E,t_1) &= \langle\langle c_\sigma(t);c^{\dagger}_{\sigma}(t_1)\rangle\rangle \\ &= -\mathrm{i}\int_{t_1}^{\infty}\langle\{c_\sigma(t);c^{\dagger}_{\sigma}(t_1)\}\rangle\,\mathrm{e}^{\mathrm{i}E(t-t_1)}\,\mathrm{d}t. \end{aligned}$$

When the coupling $\tau_{\gamma\beta\sigma}$ in the Hamiltonian (1) is time-dependent, and E_0 and $\epsilon_{\gamma\beta\sigma}$ are time-independent, we can deduce the following formulae:

$$\begin{aligned} \mathrm{i}\frac{\partial G^{\gamma}_{\sigma}(t,t_1)}{\partial t} &= \delta(t-t_1)+E_0G^{\gamma}_{\sigma}(t,t_1)+\sum_{\gamma\beta}\tau_{\gamma\beta\sigma} \\ &\quad -\mathrm{i}\Theta(t-t_1)\langle c_{\gamma\beta\sigma}(t)c^{\dagger}_{\sigma}(t_1)+c^{\dagger}_{\sigma}(t_1)c_{\gamma\beta\sigma}(t)\rangle \\ &\quad -\mathrm{i}\theta(t-t_1)U\langle n_{-\sigma}c_\sigma(t)c^{\dagger}_{\sigma}(t_1) \\ &\quad +c^{\dagger}_{\sigma}(t_1)n_{-\sigma}c_\sigma(t)\rangle, \end{aligned}$$

and

$$\frac{\partial G^{\gamma}_{\sigma}(t,t_1)}{\partial t} = -\frac{\mathrm{i}}{2\pi}\int EG^{\gamma}_{\sigma}(E,t_1)\,\mathrm{e}^{-\mathrm{i}E(t-t_1)}\,\mathrm{d}E.$$

Then, with the Fourier transform, and letting $\widehat{f}$ denote the inverse Fourier transform of f and $g*h$ denote the convolution of g and h, we get

$$\begin{aligned} EG^{\gamma}_{\sigma}(E,t_1) &= 1+\sum_{\gamma\beta}\widehat{\tau_{\gamma\beta\sigma}}*\langle\langle c_{\gamma\beta\sigma};c^{\dagger}_{\sigma}\rangle\rangle+E_0G^{\gamma}(E,t_1) \\ &\quad +U\langle\langle n_{-\sigma}c_\sigma;c^{\dagger}_{\sigma}\rangle\rangle, \end{aligned}$$

and

$$\begin{aligned} (E-E_0)\langle\langle c_\sigma;c^{\dagger}_{\sigma}\rangle\rangle &= 1+\sum_{\gamma\beta}\widehat{\tau_{\gamma\beta\sigma}}*\langle\langle c_{\gamma\beta\sigma};c^{\dagger}_{\sigma}\rangle\rangle \\ &\quad +U\langle\langle n_{-\sigma}c_\sigma;c^{\dagger}_{\sigma}\rangle\rangle, \end{aligned}$$

which is Eq. (2) in the main text.

Similarly, $\langle\langle c_{\gamma\beta\sigma};c^{\dagger}_{\sigma}\rangle\rangle$ obeys the equation

$$(E-\epsilon_{\gamma\beta\sigma})\langle\langle c_{\gamma\beta\sigma};c^{\dagger}_{\sigma}\rangle\rangle = \widehat{\tau_{\gamma\beta\sigma}}*\langle\langle c_\sigma;c^{\dagger}_{\sigma}\rangle\rangle,$$

which is Eq. (3).

Finally, $\langle\langle n_{-\sigma}c_\sigma;c^{\dagger}_{\sigma}\rangle\rangle$ satisfies

$$\begin{aligned} &(E-E_0-U)\langle\langle n_{-\sigma}c_\sigma;c^{\dagger}_{\sigma}\rangle\rangle \\ &= \langle n_{-\sigma}\rangle+\sum_{\gamma\beta}\Big\{\widehat{\tau_{\gamma\beta\sigma}}*\langle\langle c_{\gamma\beta\sigma}n_{-\sigma};c^{\dagger}_{\sigma}\rangle\rangle \\ &\quad +\widehat{\tau_{\gamma\beta-\sigma}}*\langle\langle c^{\dagger}_{-\sigma}c_{\gamma\beta-\sigma}c_\sigma;c^{\dagger}_{\sigma}\rangle\rangle \\ &\quad -\widehat{\tau^{*}_{\gamma\beta-\sigma}}*\langle\langle c^{\dagger}_{\gamma\beta-\sigma}c_{-\sigma}c_\sigma;c^{\dagger}_{\sigma}\rangle\rangle\Big\}, \end{aligned}$$

with

$$\begin{aligned} &(E-\epsilon_{\gamma\beta\sigma})\langle\langle c_{\gamma\beta\sigma}n_{-\sigma};c^{\dagger}_{\sigma}\rangle\rangle \\ &= \widehat{\tau^{*}_{\gamma\beta\sigma}}*\langle\langle n_{-\sigma}c_\sigma;c^{\dagger}_{\sigma}\rangle\rangle \\ &\quad +\sum_{\gamma'\beta}\Big\{\widehat{\tau_{\gamma'\beta-\sigma}}*\langle\langle c_{\gamma\beta\sigma}c^{\dagger}_{-\sigma}c_{\gamma'\beta-\sigma};c^{\dagger}_{\sigma}\rangle\rangle \\ &\quad -\widehat{\tau^{*}_{\gamma'\beta-\sigma}}*\langle\langle c^{\dagger}_{\gamma'\beta-\sigma}c_{-\sigma}c_{\gamma\beta\sigma};c^{\dagger}_{\sigma}\rangle\rangle\Big\}, \\ &(E-\epsilon_{\gamma\beta-\sigma})\langle\langle c^{\dagger}_{-\sigma}c_{\gamma\beta-\sigma}c_\sigma;c^{\dagger}_{\sigma}\rangle\rangle \\ &= \widehat{\tau^{*}_{\gamma\beta-\sigma}}*\langle\langle n_{-\sigma}c_\sigma;c^{\dagger}_{\sigma}\rangle\rangle \\ &\quad -\sum_{\gamma'\beta}\Big\{\widehat{\tau_{\gamma'\beta-\sigma}}*\langle\langle c^{\dagger}_{\gamma'\beta-\sigma}c_{\gamma\beta-\sigma}c_\sigma;c^{\dagger}_{\sigma}\rangle\rangle \\ &\quad +\widehat{\tau_{\gamma'\beta\sigma}}*\langle\langle c^{\dagger}_{-\sigma}c_{\gamma\beta-\sigma}c_{\gamma'\beta\sigma};c^{\dagger}_{\sigma}\rangle\rangle\Big\}, \end{aligned}$$

and

$$\begin{aligned} &(E-2E_0-U+\epsilon_{\gamma\beta-\sigma})\langle\langle c^{\dagger}_{\gamma\beta-\sigma}c_{-\sigma}c_\sigma;c^{\dagger}_{\sigma}\rangle\rangle \\ &= -\widehat{\tau_{\gamma\beta-\sigma}}*\langle\langle n_{-\sigma}c_\sigma;c^{\dagger}_{\sigma}\rangle\rangle \end{aligned}$$

$$+\sum_{\gamma'\beta}\left\{\widehat{\tau_{\gamma'\beta\sigma}} * \langle\langle c^{\dagger}_{\gamma'\beta-\sigma}c_{-\sigma}c_{\gamma\beta\sigma};c^{\dagger}_{\sigma}\rangle\rangle\right.$$
$$\left.-\widehat{\tau_{\gamma'\beta-\sigma}} * \langle\langle c^{\dagger}_{\gamma\beta-\sigma}c_{\sigma}c_{\gamma'\beta-\sigma};c^{\dagger}_{\sigma}\rangle\rangle\right\}.$$

By omitting the average terms such as $\langle c^{\dagger}_{\sigma}c_{\gamma\beta\sigma}\rangle$ and also using[31]

$$\langle c^{\dagger}_{\gamma\beta\sigma}c_{\gamma'\beta\sigma}\rangle = \langle c_{\gamma'\beta\sigma}c^{\dagger}_{\gamma\beta\sigma}\rangle = \delta_{\gamma\gamma'}f^{\beta}_{\gamma\sigma},$$

and[36]

$$\langle\langle A^{\dagger}BC;D^{\dagger}\rangle\rangle \approx \langle A^{\dagger}B\rangle\langle\langle C;D^{\dagger}\rangle\rangle - \langle A^{\dagger}C\rangle\langle\langle B;D^{\dagger}\rangle\rangle,$$

we can obtain Eq. (4).

References

[1] Kastner M A 1992 *Rev. Mod. Phys.* **64** 849
[2] Ng T K and Lee P A 1988 *Phys. Rev. Lett.* **61** 1768
[3] Hershfield S, Davies J H and Wilkins J W 1991 *Phys. Rev. Lett.* **67** 3720
[4] Zhang G M and Yu L 2007 *Physics* **36** 434 (in Chinese)
[5] Hettler M H, Kroha J and Hershfield S 1994 *Phys. Rev. Lett.* **73** 1967
[6] Ralph D C and Buhrman R A 1992 *Phys. Rev. Lett.* **69** 2118
[7] Hershfield S, Davies J H and Wilkins J W 1992 *Phys. Rev. B* **46** 7046
[8] Scheible D V, Weiss C, Kotthaus J P and Blick R H 2004 *Phys. Rev. Lett.* **93** 186801
[9] Erbe A, Weiss C, Zwerger W and Blick R H 2001 *Phys. Rev. Lett.* **87** 096106
[10] Mravlje J and Ramsak A 2008 *Phys. Rev. B* **78** 235416
[11] Shekhter R I, Gorelik L Y, Krive I V, Kiselev M N, Parafilo A V and Jonson M 2013 *Nanoelectromechanical Systems* **1** 1
[12] Zhang J H, Mao X L, Liu Q Q, Gu F, Li M, Liu H and Ge Y X 2012 *Chin. Phys. B* **21** 086101
[13] Kim C, Prada M and Blick R H 2012 *ACS Nano* **6** 651
[14] Wang R Q, Wang B G and Xing D Y 2008 *Phys. Rev. Lett.* **100** 117206
[15] Kiselev M N, Kikoin K, Shekhter R I and Vinokur V M 2006 *Phys. Rev. B* **74** 233403
[16] Donarini A, Novotny T and Jauho A P 2005 *New J. Phys.* **7** 237
[17] Tahir M and MacKinnon A 2011 arXiv:1105.5614v1
[18] Meir Y and Wingreen N S 1992 *Phys. Rev. Lett.* **68** 2512
[19] Costi T A, Schmitteckert P, Kroha J and Wolfle P 1994 *Phys. Rev. Lett.* **73** 1275
[20] Arrachea L 2007 *Phys. Rev. B* **75** 035319
[21] Cornaglia P S, Usaj G and Balseiro C A 2007 *Phys. Rev. B* **76** 241403
[22] Wingreen N S and Meir Y 1994 *Phys. Rev. B* **49** 11040
[23] Aguado R and Langreth D C 2003 *Phys. Rev. B* **67** 245307
[24] Hettler M H and Schoeller H 1995 *Phys. Rev. Lett.* **74** 4907
[25] Wu B H and Cao J C 2010 *Phys. Rev. B* **81** 085327
[26] Liu D E, Burdin S and Baranger H U 2012 arXiv:1210.4349
[27] Arrachea L 2005 *Phys. Rev. B* **72** 125349
[28] Jauho A P, Wingreen N S and Meir Y 1994 *Phys. Rev. B* **50** 5528
[29] Meir Y, Wingreen N S and Lee P A 1993 *Phys. Rev. Lett.* **70** 2601
[30] Fazio R and Raimondi R 1998 *Phys. Rev. Lett.* **80** 2913
[31] Zinbovskaya N A 2008 *Phys. Rev. B* **78** 035331
[32] Meir Y, Wingreen N S and Lee P A 1991 *Phys. Rev. Lett.* **66** 3048
[33] Liang W, Shores M P, Bockrath M, Long J R and Park H 2002 *Nature* **417** 725
[34] Roch N, Florens S, Bouchiat V, Wernsdorfer W and Balestro F 2008 *Nature* **453** 633
[35] Park H, Park J, Lim A K L, Anderson E H, Alivisatos A P and McEuen P L 2000 *Nature* **407** 57
[36] Kashcheyevs V, Aharony A and Entin-Wohlman O 2006 *Phys. Rev. B* **73** 125338